Polarization-extinction-based detection of DNA hybridization *in situ* using a nanoparticle wire-grid polarizer

Hojeong Yu,[1] Youngjin Oh,[1] Soowon Kim,[2] Seok Ho Song,[2] and Donghyun Kim[1,*]

[1]*School of Electrical and Electronic Engineering, Yonsei University, Seoul 120-749, South Korea*

[2]*Department of Physics, Hanyang University, Seoul 133-791, South Korea*

**Corresponding author: kimd@yonsei.ac.kr*

Received July 10, 2012; revised July 31, 2012; accepted July 31, 2012; posted July 31, 2012 (Doc. ID 172114); published September 14, 2012

Metallic wires can discriminate light polarization due to strong absorption of electric fields oscillating in parallel to wires. Here, we explore polarization-based biosensing of DNA hybridization *in situ* by employing metal target-conjugated nanoparticles to form a wire-grid polarizer (WGP) as complementary DNA strands hybridize. Experimental results using gold nanoparticles of 15 nm diameter to form a WGP of 400 nm period suggest that polarization extinction can detect DNA hybridization with a limit of detection in the range of 1 nM concentration. The sensitivity may be improved by more than an order of magnitude if larger nanoparticles are employed to define WGPs at a period between 400 and 500 nm.

OCIS codes: 120.1880, 230.5440, 280.1415.

Numerous optical sensor platforms have been developed to monitor and quantify biomolecular interactions in real time, including approaches that use fluorescence labeling, surface plasmon resonance (SPR), and waveguide, resonant cavity, or whispering gallery modes [1–5]. Here, we explore biomolecular sensing based on light polarization changes. A key component of this scheme is a wire-grid polarizer (WGP), which is a polarization-sensitive element used in various applications, because of its planarity and excellent polarization performance [6–15]. Periodic wire grids of a WGP are made of good conductor; electric fields parallel to the wire grids (TE polarization) are absorbed and not maintained. The field strength of TE polarization thus becomes much smaller than that of TM, whose electric field is orthogonal to the wires. In other words, an electric field oscillates orthogonally to grating wires as the light is transmitted through a WGP.

In this Letter, we employ a nanoparticle (NP)-based WGP (NP-WGP) by forming a WGP with metal NPs that are conjugated with target biomolecules. As a target biomolecular interaction mediated by NPs progresses, polarimetric extinction by a NP-WGP, which is measured by polarization extinction ratio (ER), defined as T_{TM}/T_{TE} (T_{TM} and T_{TE} are respectively transmittance for TM and TE polarization components), increases and thus can indicate the degree of an interaction on a quantitativebasis. The overall concept was attempted for detecting higher-order diffraction efficiency in the course of hybridization of NP-conjugated DNAs [16]. In contrast to commercial WGPs with metal wire grids that are at least a few hundred nanometers thick, polarization extinction in this case is provided by metal nanoparticles that are smaller than 100 nm in diameter. For this reason, the ER of a NP-WGP tends to be low. After assuming that tightly packed gold NPs (GNPs) with 15 nm diameter form 200 nm wide periodic wires on a 40 nm thick gold film and that the wires are separated by polymer of the same width, that is, a WGP of a 400 nm period (Λ) at 50% fill factor (f), numerical evaluation of ER using rigorous coupled wave analysis (RCWA) shows that the expected ER is approximately 1.17. The goal of this Letter, therefore, is to confirm the ER experimentally and to explore whether it may be sufficient to detect biomolecular interactions and, more interestingly, how it may be improved. Potential advantages of using NP-WGPs for detecting biomolecular interactions include the simplicity of required optical configurations that consist of inexpensive optical components without the need for any scanning and the possibility of high-throughput measurements because the detection can be performed in an extremely large array.

Construction of an NP-WGP was begun with evaporation of 2 nm thick chrome and 40 nm gold on an SF10 glass substrate. Negative electron-beam resist (AR-N 7520, Allresist GmbH, Strausberg, Germany) was spin-coated and patterned at $\Lambda = 400$ nm using e-beam lithography. A resist polymer grating structure was obtained after development. Single-stranded DNA (ssDNA) molecules were thiolated and adsorbed preferentially onto the exposed gold surface.

Two polyacrylamide gel electrophoresis (PAGE)-purified DNA oligomers (24-mers) modified with amine and thiol were purchased from Bioneer Corporation (Daejeon, Korea) as a capture probe single-stranded DNA (C-ssDNA) and a target probe single-stranded DNA (T-ssDNA). Thiol was attached at the 5′-end terminal of C-ssDNA and amine was attached for T-ssDNA with the following sequence: thiol-5′-TTT TTT CGG TAT GCA TGC CAT GGC-3′ for C-ssDNA and amine-5′-GCC ATG GCA TGC ATA CCG AAA AAA-3′ for T-ssDNA. C-ssDNA and T-ssDNA were complementary for hybridization. All stock oligonucleotide solutions were stored at –20 °C and made with deionized distilled water.

For immobilization of C-ssDNA at an increased cohesion efficiency, the gold surface was first treated using a plasma cleaner (Harrick Scientific Products, Pleasantville, New York, USA) for 5 min. Also, dithiothreitol and ethyl acetate were used to improve covalent linkage of the thiol-labeled C-ssDNA. A C-ssDNA layer was formed on the gold surface by immersing a polymer grating sample in 1 μM C-ssDNA mixed with 1 M KH_2PO_4 as an

immobilization buffer for 6 h at 4 °C. Subsequently, the grating sample was washed with TE buffer (10 mM Tris-HCl, 1 m Methylenediaminetetraacetic acid: EDTA, pH 7.6) for 5 min and was treated in 1 mM 6-mercapto-1-hexanol (MCH, Sigma-Aldrich, St. Louis, MO, USA) in ethanol for 1 h to increase hybridization efficiency. By using an ethanol-in-buffer solution, negative e-beam resist was melted away, leaving only C-ssDNA and MCH groups on the gold surface patterned in a grating structure.

For cross-linking between T-ssDNA and GNPs, carboxyl polyethylene glycol (PEG) conjugated spherical GNPs ($\phi = 15$ nm, <20% coefficient of variation, Polysciences Inc., Pennsylvania, USA) were prepared with carboxyl terminal groups, which were cross-linked with amines positioned at the 5′-end terminal of the T-ssDNA. Throughout the experiment, the number of GNPs was maintained at 1.2×10^{12} NPs. To assist cross-linking, carbodiimide cross-linking reagents 1-ethyl-3(3′-dimethylaminopropyl)-carbodiimide (EDC, Sigma-Aldrich, St. Louis, Missouri, USA) was used, where N-hydroxysulfosucciniimide (NHS) was added for stable activation, and incubated at 4 °C for 5 h.

For hybridization, a C-ssDNA grating sample was immersed in 1 M NaCl hybridization buffer with T-ssDNA and incubated at room temperature. Polarization-extinction measurement was performed *in situ* every 30 min. The DNA-based NP-WGP was rinsed by TE buffer to remove residue T-ssDNA in the solution after hybridization. The effect of nonspecific adsorption of ssDNA onto the gold surface and physisorption of NPs to polymer residues on ER is estimated to be less than 20%. The overall scheme of NP-WGP fabrication is presented in Fig. 1(a). Figure 1(b) is a scanning electron microscopy (SEM) image of a final NP-WGP at 100 nM of T-ssDNA and shows polymer residues that were not washed away after rinsing and physisorption of NPs.

Polarimetric detection of NP-WGPs was based on a polarizer-analyzer system where light from a He–Ne laser (05-LHP-991, 10 mW, 632.8 nm, Melles-Griot, Carlsbad, CA) is polarized at 45° with respect to the horizontal plane and passes through a polarizer (Edmund Optics, Barrington, New Jersey) which polarizes incoming light either at 0° (TM) or 90° (TE). The NP-WGP sample is mounted on a custom-made dish with a hole through which light is transmitted. After an analyzer, light is filtered and detected by a photomultiplier tube (PMT, #77360, Newport, Irvine, California). Identical measurements were conducted at least three times for statistical averaging.

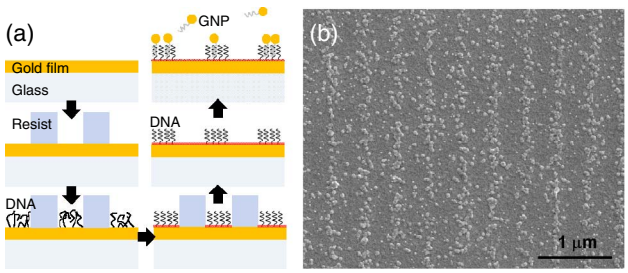

Fig. 1. (Color online) (a) Schematics of NP-WGP fabrication. (b) SEM image of a final NP-WGP sample ($\Lambda = 400$ nm).

The results are shown in Fig. 2 and suggest that DNA hybridization dynamics begin with a rapid increase and saturate eventually. Although T-ssDNA concentration ($C_{\text{T-ssDNA}}$) was varied to measure target-concentration-dependent dynamics, it is the number of total T-ssDNA molecules accessing probe DNAs that is varied under a static experimental environment. The measured time dynamics was found to follow the rate law $\text{ER}(t) = \text{ER}_\infty - (\text{ER}_\infty - \text{ER}_0)\exp(-kt)$ with good precision, as shown in Fig. 2(a). ER_∞ and ER_0 represent the saturated and initial values of ER. k is the rate constant. The variation of ER_∞ in response to T-ssDNA concentration exhibits the target-limited nature of the measured dynamics. Even if DNA hybridization was performed under a microfluidic environment, we expect that ER_∞ would be dependent on $C_{\text{T-ssDNA}}$ following the Langmuir model. The rate constant k was measured to be 1.68, 0.283, and 0.281 /h for $C_{\text{T-ssDNA}} = 1000$, 100, and 10 nM; that is, the hybridization dynamics slow quickly as $C_{\text{T-ssDNA}}$ decreases. Under low concentration, k changes little. In other words, ER_∞ is little affected by the target concentration when it is too low or too high: at low concentration, nonextinction effects tend to dominate ER, while the contribution of an NP becomes less significant after a certain concentration because ER is affected more by the diameter of NPs rather than by the grating formation. ER_∞ at high levels of T-ssDNA could be explained also by the saturation of the probes, as more T-ssDNA binds to each GNP. Figure 2(b) shows ER_∞ with respect to $C_{\text{T-ssDNA}}$. Effectively, Fig. 2(b) is an isotherm that presents the dynamic range of detection based on NP-WGP as $C_{\text{T-ssDNA}} = 1 \sim 1,000$ nM. If we define the limit of detection (LOD)

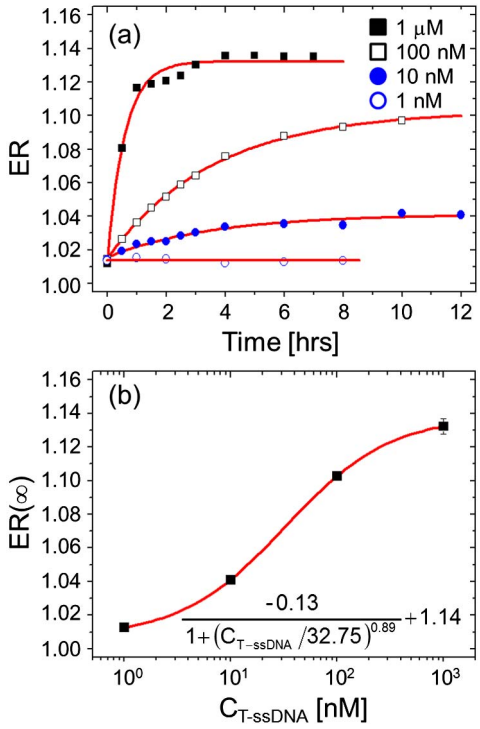

Fig. 2. (Color online) (a) DNA hybridization dynamics with time for various T-ssDNA concentrations. (b) ER at saturation for different target concentration and fitted to a sigmoidal statistic.

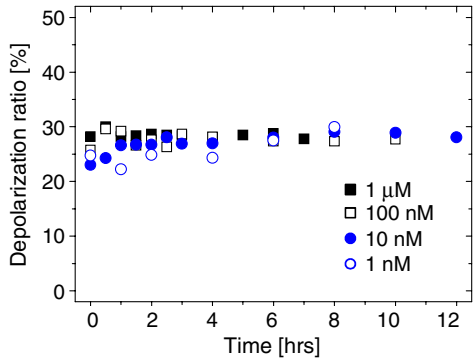

Fig. 3. (Color online) Measured depolarization during the NP-WGP-mediated DNA hybridization with T-ssDNA concentration.

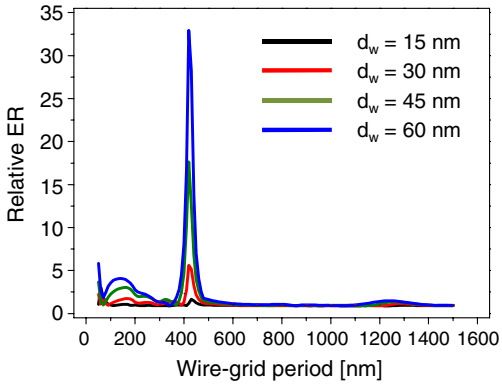

Fig. 4. (Color online) Relative ERs assuming that GNPs form perfect WGPs at $f = 50\%$ in reference to the result of $\Lambda = 400$ nm. Wire-grid thickness (d_w) represents the diameter of GNPs.

as the $C_{\text{T-ssDNA}}$ at which extinction contrast reaches one-tenth of the maximum, LOD is approximately 3 nM.

One may argue that the extinction characteristics may be significantly affected by the scattering of GNPs. The scattering by GNPs can be described by Rayleigh scattering that is associated with single scatterers. However, according to this single-scatterer-based Rayleigh scattering, the input polarization remains largely unchanged, and thus depolarization by the GNPs should be negligible at normal incidence. For experimental characterization of scattering, we have introduced a depolarization ratio that is defined as the intensity ratio of depolarized to transmitted light. The depolarization ratio was extracted from the Jones calculus that was used to model the polarization of NP-WGP. Figure 3 shows that the depolarization ratio is approximately constant under 30% throughout DNA hybridization, although slight variation is observed at the beginning. In other words, measured depolarization is not associated with GNP scattering. Potential mechanisms that may be responsible for the depolarization include polymer residues and scattering centers on the surface of gold film due to roughening after polymer development and MCH treatment. Although depolarization was significant and may reduce signal-to-noise ratio, its effect on the measurement of NP-WGP seems minimal.

For practical applications of NP-WGP for biosensing, an important challenge is to achieve low LOD while increasing the dynamic range. For example, optical detection based on SPR works well for large molecules typically at concentrations of 100 pM. One way of addressing the challenge is to employ large GNPs and to create WGPs at a period optimized for enhanced detection. Figure 4 shows the numerically calculated improvement of ERs relative to the case of NP-WGP at $\Lambda = 400$ nm. The calculation is based on two-dimensional RCWA assuming $f = 50\%$ and wire-grid thickness (d_w) equal to GNP diameter. In Fig. 4, the relative ER higher than one indicates enhancement. It is suggested that GNPs larger than 30 nm can be used for significant enhancement of ER, though increased scattering may reduce signal-to-noise ratio. Virtually no enhancement was observed except for NP-WGPs with a period between 400 and 500 nm. For GNPs with $\phi = 45$ and 60 nm, the highest enhancement was obtained as 33 and 18, when the GNPs form wire-grids at $\Lambda = 420$ nm in both cases. In other words, the enhancement of LOD by an order of magnitude should be achievable based on NP-WGP, which can be combined with other approaches, for instance in a sandwiched assay with NPs, for further enhancement of LOD.

In summary, we report the polarization-based detection of DNA hybridization *in situ* by forming DNA-conjugated GNPs into WGPs. Experimentally obtained LOD was on the order of 1 nM. Further improvement by more than an order is expected by employing larger NPs and optimizing the parameters of wire-grids formed with NPs.

This work was supported by the National Research Foundation (NRF) grants funded by the Korean government (2010-0007993 and 2011-0017500).

References

1. S. W. Thomas, G. D. Joly, and T. M. Swager, Chem. Rev. **107**, 1339 (2007).
2. H. Baac, J. P. Hajos, J. Lee, D. Kim, S. J. Kim, and M. L. Shuler, Biotechnol. Bioeng. **94**, 815 (2006).
3. S. Moon, Y. Kim, Y. Oh, H. Lee, H. C. Kim, K. Lee, and D. Kim, Biosens. Bioelectron. **32**, 141 (2012).
4. R. Horváth, H. C. Pedersen, N. Skivesen, D. Selmeczi, and N. B. Larsen, Opt. Lett. **28**, 1233 (2003).
5. F. Vollmer and S. Arnold, Nat. Methods **5**, 591 (2008).
6. H. Tamada, T. Doumuki, T. Yamaguchi, and S. Matsumoto, Opt. Lett. **22**, 419 (1997).
7. S. Arnold, E. Gardner, D. Hansen, and R. Perkins, in *SID 01 Digest* (Society for Information Display, 2001), p. 1282.
8. D. Kim, C. Warde, K. Vaccaro, and C. Woods, Appl. Opt. **42**, 3756 (2003).
9. D. Kim, Appl. Opt. **44**, 1366 (2005).
10. S. H. Kim, J.-D. Park, and K.-D. Lee, Nanotechnology **17**, 4436 (2006).
11. V. Pelletier, K. Asakawa, M. Wu, D. H. Adamson, R. A. Register, and P. M. Chaikin, Appl. Phys. Lett. **88**, 211114 (2006).
12. L. Chen, J. J. Wang, F. Walters, X. Deng, M. Buonanno, S. Tai, and X. Liu, Appl. Phys. Lett. **90**, 063111 (2007).
13. D. Crouse and P. Keshavareddy, Opt. Express **15**, 1415 (2007).
14. Ö. Sepsi, I. Szanda, and P. Koppa, Opt. Express **18**, 14547 (2010).
15. I. Yamada, N. Yamashita, K. Tani, T. Einishi, M. Saito, K. Fukumi, and J. Nishii, Opt. Lett. **36**, 3882 (2011).
16. I. E. Sendroiu and R. M. Corn, Biointerphases **3**, FD23 (2008).